Mutations of *GPR126* Are Responsible for Severe Arthrogryposis Multiplex Congenita

Gianina Ravenscroft,[1,17] Flora Nolent,[2,3,17] Sulekha Rajagopalan,[4] Ana M. Meireles,[5] Kevin J. Paavola,[5] Dominique Gaillard,[6] Elisabeth Alanio,[7] Michael Buckland,[8,9] Susan Arbuckle,[10] Michael Krivanek,[10] Jérome Maluenda,[2,3] Stephen Pannell,[1] Rebecca Gooding,[11] Royston W. Ong,[1] Richard J. Allcock,[12] Ellaine D.F. Carvalho,[13,14] Maria D.F. Carvalho,[13,14,15] Fernando Kok,[16] William S. Talbot,[5] Judith Melki,[2,3,18,*] and Nigel G. Laing[1,18,*]

Arthrogryposis multiplex congenita is defined by the presence of contractures across two or more major joints and results from reduced or absent fetal movement. Here, we present three consanguineous families affected by lethal arthrogryposis multiplex congenita. By whole-exome or targeted exome sequencing, it was shown that the probands each harbored a different homozygous mutation (one missense, one nonsense, and one frameshift mutation) in *GPR126*. *GPR126* encodes G-protein-coupled receptor 126, which has been shown to be essential for myelination of axons in the peripheral nervous system in fish and mice. A previous study reported that $Gpr126^{-/-}$ mice have a lethal arthrogryposis phenotype. We have shown that the peripheral nerves in affected individuals from one family lack myelin basic protein, suggesting that this disease in affected individuals is due to defective myelination of the peripheral axons during fetal development. Previous work has suggested that autoproteolytic cleavage is important for activating GPR126 signaling, and our biochemical assays indicated that the missense substitution (p.Val769Glu [c.2306T>A]) impairs autoproteolytic cleavage of GPR126. Our data indicate that GPR126 is critical for myelination of peripheral nerves in humans. This study adds to the literature implicating defective axoglial function as a key cause of severe arthrogryposis multiplex congenita and suggests that *GPR126* mutations should be investigated in individuals affected by this disorder.

Arthrogryposis multiplex congenita (AMC) is a heterogeneous group of disorders defined by the presence of congenital non-progressive contractures of at least two major joints.[1,2] The incidence of AMC is ~1 in 3,000.[3] AMC can arise as part of a syndromic condition or as a result of environmental factors, such as intrauterine restriction. Non-syndromic or isolated AMC arises as a result of reduced or absent fetal movements, which can result in a range of defects, including pterygia, pulmonary hypoplasia, and craniofacial defects. AMC can overlap with other disorders, including lethal (OMIM: 253290) and non-lethal (Escobar variant [OMIM: 265000]) multiple pterygium syndromes, lethal congenital contracture syndromes, and spinal muscular atrophy type 1 (OMIM: 253300).[2] At the milder end of the spectrum are the distal arthrogryposes, in which contractures occur across the distal joints exclusively.[2] Isolated AMC phenotypes arise as a result of mutations in genes encoding components required for (1) motor neuron structure, function, and myelination (*ADCY6* [OMIM: 600294], *CNTNAP1* [OMIM: 602346], *ECEL1* [OMIM: 605896], *ERBB3* [OMIM: 190151], *GLE1* [OMIM: 603371], *PIP5K1C* [OMIM: 606102], *SMN1* [OMIM: 600354], and *TRPV4* [OMIM: 605427]), (2) the neuromuscular junction (*CHAT* [OMIM: 118490], *CHRNA1* [OMIM: 100190], *CHRNB1* [OMIM: 100710], *CHRND* [OMIM: 100720], *CHRNG* [OMIM: 100730], *CNTN1* [OMIM: 600016], *DOK7* [OMIM: 610285], *RAPSN* [OMIM: 601592], and *ZBTB42* [OMIM: 613915]), or (3) skeletal muscle (*ACTA1* [OMIM: 102610], *DMPK* [OMIM: 605377], *KLHL40* [OMIM: 615340], *KLHL41* [OMIM: 607701], *MYBPC1* [OMIM: 160794], *MYH2* [OMIM: 160740], *MYH3* [OMIM: 160720], *MYH8* [OMIM: 160741], *NEB* [OMIM: 161650], *PIEZO2* [OMIM: 613629], *RYR1* [OMIM: 180901], *SYNE1* [OMIM: 608441], *TNNI2* [OMIM: 191043], *TNNT3* [OMIM: 600692], *TPM2* [OMIM: 190990], and *TTN* [OMIM: 188840]).[4–7] Thus, isolated AMCs represent a large group of diseases arising from primary defects of the neuromuscular axis. Despite the large number of known disease-associated genes, many cases of AMC remain without a genetic diagnosis.

The families in this study provided written informed consent for genetic analysis of their babies and themselves

[1]Harry Perkins Institute of Medical Research, Centre for Medical Research, University of Western Australia, Nedlands, WA 6009, Australia; [2]Unité Mixte de Recherche-1169, INSERM, le Kremlin-Bicêtre 94276, France; [3]University Paris-Sud, le Kremlin-Bicêtre 94276, France; [4]Department of Clinical Genetics, Liverpool Hospital, Liverpool, NSW 1871, Australia; [5]Department of Developmental Biology, Stanford University, Stanford, CA 94305, USA; [6]Genetics Department, Maison Blanche Hospital, Centre Hospitalier Universitaire de Reims, Reims 51092, France; [7]Pol Bouin Laboratory, University Hospital, Reims 51092, France; [8]Brain & Mind Research Institute, University of Sydney, Sydney, NSW 2006, Australia; [9]Department of Neuropathology, Royal Prince Alfred Hospital, Camperdown, NSW 2050, Australia; [10]Department of Pathology, The Children's Hospital at Westmead, Locked Bag 4001, Westmead, NSW 2145, Australia; [11]Department of Diagnostic Genomics, PathWest Laboratory Medicine, Nedlands, WA 6009, Australia; [12]Lotterywest State Biomedical Facility Genomics, School of Pathology and Laboratory Medicine, University of Western Australia, Nedlands, WA 6009, Australia; [13]Christus University Center, Fortaleza, CE, 04013-000, Brazil; [14]Genpharma Consultoria Farmaceutica e Genetica, Ltda, Fortaleza, CE 60160-230, Brazil; [15]Ceará State University, Fortaleza, CE 04013-000, Brazil; [16]Mendelics Genomic Analysis, Sao Paulo, SP 04013-000, Brazil
[17]These authors contributed equally to this work
[18]These authors contributed equally to this work
*Correspondence: judith.melki@inserm.fr (J.M.), nigel.laing@perkins.uwa.edu.au (N.G.L.)
http://dx.doi.org/10.1016/j.ajhg.2015.04.014.

in accordance with the ethical standards of the relevant institutional review boards.

In family 1, a fetus (IV:1) was born with AMC to consanguineous parents (see pedigree in Figure S1A). An ultrasound examination detected distal joint contractures, including talus valgus and wrist and finger flexion, a diaphragmatic defect, and reduced fetal mobility from 20 weeks of gestation. The pregnancy was terminated at 20 weeks of gestation. Fetopathological examination of the aborted fetus confirmed that the joint retractions were associated with pterygium of the right elbow and axilla (Figures S1D–S1F). The diaphragmatic cupolae were thin and elevated. Brain and spinal-cord examinations were normal. Bone X-ray was normal.

In family 2, a female newborn (IV:1) was the first and only child of a first-cousin healthy couple with no family history of congenital abnormalities (see pedigree in Figure S1B). Their common ancestor has a Portuguese ethnic background. An antenatal ultrasound performed at 16 weeks of gestation disclosed upper-limb arthrogryposis, and 8 weeks later it was possible to recognize micrognathia and polyhydramnios. At 25 weeks of pregnancy, MRI revealed micrognathia and fixed extension of the arms and flexion of the elbows, wrists, and hands (Figure S2A). Intrauterine growth retardation was noted after 28 weeks of pregnancy. The fetal echocardiogram and G-band karyotype were normal.

She was born at 31 weeks of gestation by Caesarean section after premature amniorexis and had a birth weight of 1,010 g ($<3^{rd}$ percentile); birth length and occipital frontal circumference were not measured. Her Apgar score was 3 at both 1 and 5 min. Physical examination disclosed ocular hypertelorism, upper-limb arthrogryposis with ulnar deviation of the hands, camptodactyly, sparse dermal ridges, knee-joint ankylosis, and talipes equinovarus. After cardiopulmonary resuscitation and orotracheal intubation, she was transferred to an intensive care unit and given continuous adrenaline but developed severe pulmonary hypertension and died from cardiorespiratory arrest 1 hr after birth. A post-mortem blood sample was collected for DNA extraction.

In family 3, individual II:1 was born to consanguineous (second-cousin) parents of Iraqi descent and presented with AMC (see pedigree in Figure S1C). The pregnancy was complicated by polyhydramnios in the third trimester, requiring amnio-drainage. An antenatal ultrasound at 30 weeks of gestation showed intrauterine growth retardation, an absent stomach bubble, possible right-sided talipes equinovarus, and no observed upper-limb movements for over 1 hr. The antenatal karyotype was normal. Because of severe pre-eclampsia, the female infant was delivered by an emergency caesarean section at 36 weeks of gestation and died at 1 hr of life. Her birth weight was 1,190 g ($<3^{rd}$ percentile), and her Apgar scores were 2 and 5 at 1 and 5 min, respectively. Severe arthrogryposis involving large and small joints was noted, but no spontaneous limb movements were observed. She had adducted thumbs, ulnar deviation, fixed flexion contractures of the hands and wrists, and reduction of digital creases. She also showed thoracic kyphoscoliosis, bilateral severe talipes equinovarus, and generally reduced muscle bulk in the limbs. Dysmorphic facial features included a triangular face, a depressed nasal bridge, anteverted nares, a thin upper lip, micrognathia, and low-set ears. She was unable to maintain oxygenation on non-invasive ventilation, and a decision was made to withdraw resuscitation. Serum creatine kinase was normal.

The autopsy confirmed a short umbilical cord and significant pulmonary hypoplasia. Muscle histology was stated to show a diffuse non-specific myopathic picture. A quadriceps-muscle biopsy (Figures S3A and S3B) showed a biphasic distribution of muscle-fiber diameters and was composed of small rounded myofibers and hypertrophic rounded myofibers of both fiber types. Examination of other skeletal muscles, including the diaphragm, psoas, and anterior neck-strap muscles, showed significant variability in muscle-fiber diameter within each muscle. Normal and atrophic small fibers were predominant, but occasional larger hypertrophic fibers were also seen. There was patchy grouped atrophy. Both type 1 and type 2 fibers appeared atrophic on skeletal-muscle myosin staining. The most severely affected of the sampled muscles was the diaphragm (Figures S3C and S3D). Central nuclei were not markedly increased in number and were present in around 3% of diaphragm-muscle fibers overall. There was no significant endomysial or perimysial fibrosis, although focally, the fibrous septa between muscle fascicles was prominent. Immunohistochemistry was normal for spectrin, merosin, dystrophins 1–3, dysferlin, alpha-dystroglycan, laminin alpha-2, and collagen VI. There was no obvious reduction of the amount of motor neurons in the anterior horns of the spinal cord. No peripheral nerve was sampled. Other organs were essentially normal.

In family 3, individual II:2 was the second affected pregnancy, which was terminated at 19 weeks of gestation. An antenatal ultrasound scan at 18 weeks of gestation showed bilateral talipes equinovarus and probable contractures of the upper limbs, as well as no observed movements of the arms for over 1 hr. Examination showed a male fetus with arthrogryposis and poorly developed musculature of the limbs. There was bilateral severe talipes equinovarus, restricted movement of the knees and shoulders, extension contractures of the elbows, and flexion contractures of the wrists and fingers. The thumbs were adducted. Subtle dysmorphic features, including low-set ears and micrognathia, were present. The autopsy was limited to histological examination of the biceps, hamstrings, quadriceps, gastrocnemius muscles, fragments of the sural nerve, branches of the tibial and popliteal nerves, and the brachial plexus. Routine H&E examination of the muscles showed some variation in muscle-fiber diameter (mainly smaller fibers) and mildly increased perimysial fibrosis (Figures S3E and S3F). The average fiber diameter in the quadriceps was approximately 10–11 μm, but it ranged from 6–16 μm.

The amount of central nuclei and myotubules definitely increased in all muscles examined. This might reflect a delay in myofiber maturation, given that these features were not prominent in the first sibling (II:1), delivered at 36 weeks of gestation.

An X-ray babygram of individual II:2 showed multiple segmentation abnormalities of the thoracic spine, from T7–T12 (Figure S4). This was an unexpected finding, given that the babygram of individual II:1 showed no structural vertebral abnormalities, despite the presence of thoracic kyphoscoliosis. Long bones were gracile in appearance, in keeping with the lack of fetal movement.

GPR126 drives the differentiation of promyelinating Schwann cells by elevating cyclic AMP (cAMP) levels.[8] A recent study[5] showed that mutation of *ADCY6*, which encodes an adenylate cyclase that synthesizes cAMP,[9] causes AMC, suggesting that ADCY6 acts in the GPR126-cAMP pathway, which regulates myelination of Schwann cells. Therefore, *GPR126* (OMIM: 612243) was regarded as a strong candidate gene associated with human AMC and was included in a custom panel of targeted AMC-associated genes. Targeted exome sequencing was performed on the DNA sample of the affected fetus (IV:1) in family 1. The Agilent SureSelectXT Custom Kit (targeting 500 Kb, including all known AMC-associated genes and candidate genes, including *GPR126*) was used for library preparation and exome enrichment, as previously described.[5] Sequencing was performed with paired-end 75-bp reads on an Illumina MiSeq System and with the MiSeq Reagent Nano Kit v.2 according to Illumina's protocol. The average median coverage was 73. Reads were aligned to the human reference genome sequence (UCSC Genome Browser hg19, NCBI build 37.3) via the Burrows-Wheeler Aligner (BWA).[10] Variants were selected with SAMtools[11] and then annotated with ANNOVAR software.[12] Reads with a coverage of at least 2-fold were filtered against the exome data in dbSNP v.137. Of the variants with a minor allele frequency (MAF) < 0.0015, those located in coding regions or intron-exon junctions or those that were short coding insertions or deletions were selected. MAF was updated according to dbSNP v.142 and the NHLBI Exome Sequencing Project Exome Variant Server (EVS; ESP6500SI-V2). The Integrative Genomics Viewer v.1.5.64[13] was used to visualize exome sequencing variants.

For the proband of family 2 (IV:1), exome sequencing was performed with a Nextera Exome Capture Kit (Illumina) on a HiSeq 2500 sequencer (Illumina), resulting in 12 GB of sequencing. Alignment was performed with the BWA-MEM, and genotyping was performed with the Genome Analysis Toolkit v.3. Because the parents were consanguineous, special attention was paid to homozygous variants.

For the proband (II:1) from family 3, analysis with the Illumina HumanCytoSNP-12 showed no copy-number variants in the genomic DNA. However, homozygosity mapping showed long continuous stretches of homozygosity on chromosomes 3, 4, 6, 9, and 11 (collectively representing 3% of the genome), including region 4p16.3, which encompasses *DOK7*. However, targeted next-generation sequencing and Sanger sequencing of *DOK7* did not reveal any mutations. Targeted next-generation sequencing of a large number of neuromuscular genes was performed as described previously[14] and showed no significant findings. *SMN1*-related spinal muscular atrophy and myotonic dystrophy were excluded by genetic testing.

Exome enrichment was performed on DNA from the proband (with an AmpliSeq Whole Exome Kit [Thermo Fisher Scientific]). In brief, a total of 100 ng of DNA was amplified in 12 separate PCR pools, each containing ~25,000 primer pairs, under the following conditions: 99°C for 2 min followed by ten cycles of 99°C for 15 s and 60°C for 16 min. After amplification, the individual reactions were pooled and digested with the supplied enzyme, FuPa, which degraded the PCR primers. Next, barcoded sequencing adaptors were ligated, and the library was purified with AMPure beads (Beckman Coulter) and amplified with Platinum high-fidelity polymerase for five cycles. The final amplified library was purified again with AMPure beads and analyzed on a 2100 Bioanalyzer (Agilent Technologies). Libraries were diluted to 18–26 pM and attached to ion sphere particles via the Ion Proton Template 200 Kit v.3 and sequenced on a P1 sequencing chip for 520 flows on an Ion Proton sequencer (Ion Sequencing 200 Kit v.3). Two samples were pooled and sequenced on a single chip. After sequencing, reads were trimmed for the removal of low-quality bases from the 3′ end and mapped with TMap (Torrent Suite v.4.2) to the human genome reference sequence (UCSC Genome Browser hg19). Variant calling was performed with the Torrent Variant caller with custom settings optimized for whole exomes, and the data were annotated with Ion Reporter v.4.0. Variants were filtered with ANNOVAR[12] against those in ENCODE GENCODE v.19, 1000 Genomes (threshold $> 0.5\%$), dbSNP v.138, and a list of in-house common variants. After filtering, variants within the regions of homozygosity (identified by SNP array) were prioritized.

In consanguineous family 1, targeted exome sequencing identified a homozygous nonsense mutation in exon 2 of *GPR126* in fetus IV:1 (c.19C>T [p.Arg7*]; GenBank: NM_198569.2; GI: 189095282; ClinVar: SCV000222094). Sanger sequencing confirmed that this variant was homozygous in the proband (IV:1) and heterozygous in both parents (III:1 and III:2; Figure S5). This mutation was found in neither EVS (ESP6500SI-V2) nor dbSNP v.142.

Exome sequencing of the proband from family 2 (IV:1) identified a homozygous deleterious variant in exon 15 of *GPR126* (Figure S2B): c.2144dup (ClinVar: SCV000222095), which leads to a substitution of the glutamine at position 716 to threonine and causes a frameshift followed by a premature stop codon (p.Gln716Thrfs*16). Sanger sequencing (Figure S2C) confirmed the presence of this homozygous variant in the proband and showed

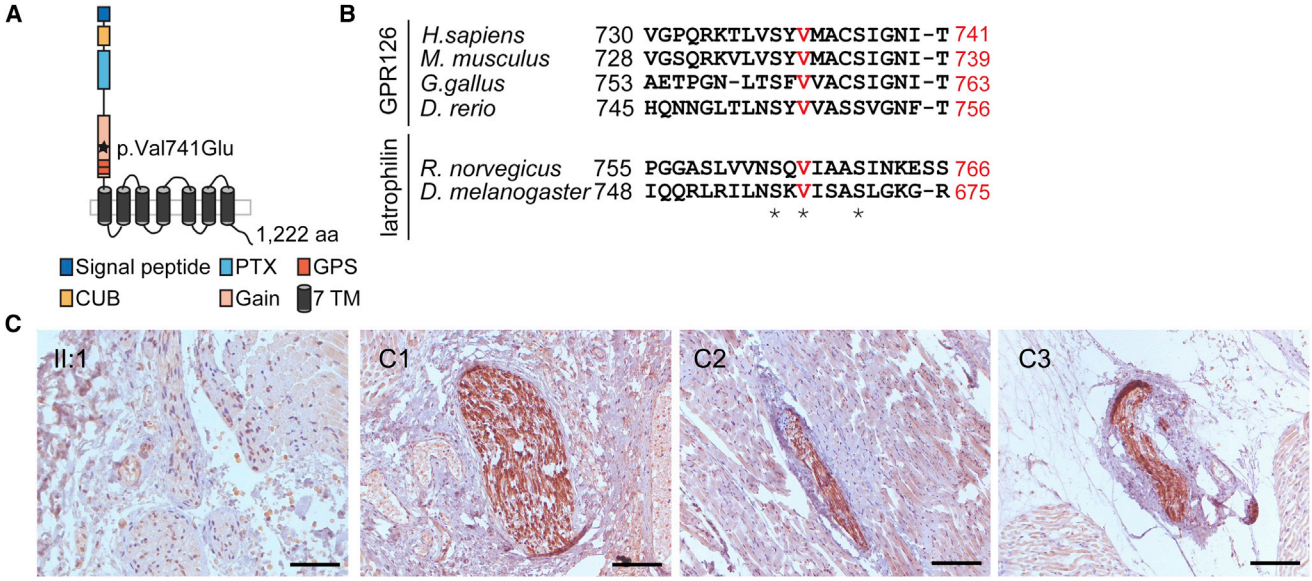

Figure 1. *GPR126* Missense Mutation Identified in Family 3 and Phenotypic Analysis
(A) Schematic representation of the human GPR126 (Ensembl: ENST00000367608) shows conserved domains and the p.Val741Glu substitution.
(B) Sequence alignment of GPR126 from different vertebrates and of latrophilin from mammals and insects shows that the substituted valine (red) is highly conserved. Sequence alignments include those of *H. sapiens* GPR126 (Ensembl: ENST00000367608), *M. musculus* Gpr126 (Ensembl: ENSMUST00000041168), *G. gallus* GPR126 (Ensembl: ENSGALT00000022408), *D. rerio* Gpr126 (GenBank: NP_001156763), *R. norvegicus* latrophilin (Ensembl: ENSRNOT00000045699), and *D. melanogaster* latrophilin (Ensembl: FBtr0310448).
(C) Immunohistochemistry of MBP in the psoas intramuscular nerve in II:1 (family 3) and three age-matched control psoas muscles (C1–C3). Scale bars represent 100 μm.

that both parents (III:1 and III:2) were heterozygous carriers.

Combining sequencing and homozygosity mapping on the proband from family 3 identified 19 homozygous variants, including a missense variant in *GPR126* (chr6: 142729324T>A). This mutation causes variants in two different *GPR126* transcripts: c.2306T>A (exon 16; ClinVar: SCV000222096; Ensembl: ENST00000367609), which results in a substitution of a highly conserved amino acid (p.Val769Glu), and c.2222T>A (p.Val741Glu) (exon 15; GenBank: NM_001032395.2; Ensembl: ENST00000367608; Figures 1A and 1B). The p.Val741Glu substitution was predicted to be deleterious by MutationTaster, PolyPhen-2, and SIFT. This variant was not present in the NHLBI Exome Sequencing Project EVS, 1000 Genomes, or the ExAC Browser (Beta; Broad Institute). Bi-directional Sanger sequencing confirmed that this variant was homozygous in the proband and the affected sibling and that each parent was a heterozygous carrier (Figure S6).

GPR126 is critical for myelination within the peripheral nervous system (PNS) during development.[8,15,16] To investigate the pathogenicity of the missense substitution identified in family 3, we examined myelination in the affected individuals' samples and performed biochemical analysis on the protein. Evaluation of the proband's psoas muscle revealed an almost complete absence of myelin basic protein (MBP) staining in the intramuscular nerves, whereas staining was present in three age-matched control samples (Figure 1C). For individual II:2, MBP staining was performed on all sampled nerves, including intramuscular nerves of the biceps muscle. Age-matched control samples were only available for the psoas intramuscular nerves. The three control samples showed patchy areas of positive MBP staining, but MBP staining was completely absent in all nerves examined in individual II:2 (Figure S7). Routine H&E staining of the intramuscular nerve fascicles in II:1 and II:2 was unremarkable in comparison to staining in normal control samples, and peripheral nerves in II:2 showed no definite abnormalities.

GPR126 is a member of the adhesion GPCR (aGPCR) family of proteins, which are characterized by a long extracellular N-terminal region and a conserved GAIN domain, in addition to the heptahelical transmembrane domain shared by all GPCRs.[17] Previous studies on GPR126 and other aGPCRs have indicated that the GAIN domain mediates an autocatalytic cleavage event that allows a "tethered agonist" peptide sequence within the receptor to activate signaling.[18–20] The mutation in family 3 replaces a valine residue that is widely conserved in GPR126 and in other aGPCRs in vertebrates and invertebrates (e.g., Figure 1B). The corresponding valine residue in the crystal structure of rat latrophilin is near the amino acids that mediate the autocatalytic cleavage.[18] To determine whether this nonconservative substitution affects receptor cleavage, we analyzed constructs containing the full-length human GPR126 sequence and a C-terminal FLAG tag (Figure 2A). The full-length constructs utilized were for transcript

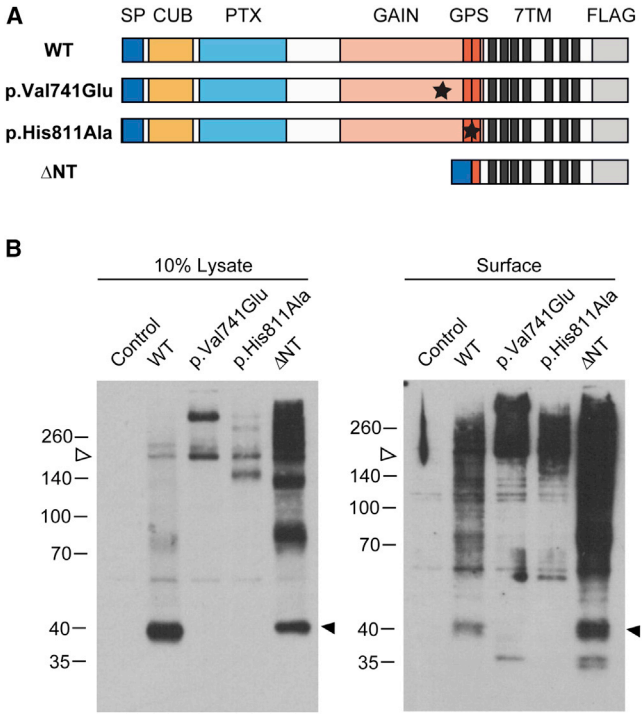

Figure 2. Functional Characterization of the p.Val741Glu Substitution in GPR126

(A) Graphical representation of FLAG-tagged human GPR126 constructs corresponding to the wild-type (WT) protein, the p.Val741Glu substitution, a variant with disruption in the catalytic triad (p.His811Ala) that mediates autoproteolysis, and a deletion construct lacking the N-terminal fragment (ΔNT).

(B) Immunoblots of samples from transfected HEK293 cells show total cell lysate (left) or surface-labeled proteins (right). The control cells were transfected with the empty expression vector. The cleaved (filled arrowhead) and uncleaved full-length (open arrowhead) proteins are noted. The autoproteolytic activity of the p.Val741Glu construct was consistently reduced, but some cleaved product was evident on long exposures. The blot shown is representative of three independent experiments.

ENST00000367608; hence, the substitution is referred to as p.Val741Glu for these functional studies. HEK293 cells transfected with vectors encoding the wild-type and p.Val741Glu proteins were analyzed in parallel with another missense substitution protein (p.His811Ala) that lacks autoproteolyic activity.[18] We also analyzed a fourth construct encoding a truncated GPR126 derivative corresponding to the C-terminal fragment of the receptor after cleavage. Cell-surface proteins were biotinylated, precipitated with streptavidin beads, and analyzed by immunoblotting with the anti-FLAG antibody as previously described.[19] The cleaved C-terminal fragment was evident in the surface fraction of the cells transfected with wild-type GPR126, but was reduced in the p.Val741Glu and p.His811Ala samples (Figure 2B). In the corresponding whole-cell lysates, the p.Val741Glu and p.His811Ala samples had a large amount of uncleaved, full-length product. These data indicate that the p.Val741Glu substitution greatly reduced autoproteolytic cleavage of GPR126 and provide further evidence that this lesion caused the AMC affecting family 3.

GPR126 is essential for myelination of axons in peripheral nerves. Evidence from studies in zebrafish, mice, and humans indicates that Gpr126 and GPR126 signal through the second messenger cAMP and protein kinase A.[16] In zebrafish *gpr126* mutants, Schwann cells arrest at the promyelinating stage.[8] Myelination has been restored in *gpr126* mutants treated with the adenylyl cyclase agonist forskolin, providing evidence that Gpr126 signaling triggers myelination by increasing cAMP levels.[8,21] In addition, cAMP levels are reduced in the nerves of *Gpr126* mutant mice, and activation of PKA can activate myelin gene expression in *gpr126* mutants.[21,22] Recently, a homozygous missense mutation in *ADCY6,* which encodes an adenylyl cyclase protein that synthesizes cAMP, was identified in a consanguineous family affected by severe AMC.[5] Ultrastructural analysis of the affected individual's nerve samples revealed the presence of Schwann cells but a lack of myelin in the PNS. Knockdown of the orthologous genes in zebrafish disrupted myelin in the PNS, producing phenotypes similar to those of the affected individuals and *gpr126* mutant zebrafish.[5] Despite the evidence that Gpr126 signaling has a conserved function in myelination in vertebrates, previous studies have not identified *GPR126* mutations that disrupt myelination in humans.

Our sequencing studies have identified homozygous *GPR126* mutations in three consanguineous families affected by lethal arthrogryposis. *Gpr126*-null mice had abnormal joint contractures of the limbs by P4 (some were affected at birth), reminiscent of AMC.[15] Similarly, the AMC affecting families 1 and 2 is caused by mutations predicted to eliminate GPR126. Our biochemical studies indicate that the p.Val741Glu substitution in family 3 impairs GPR126 cleavage (Figure 2), which is required to activate GPR126 signaling in cultured cells.[19,20] The p.Val741Glu substitution reduced but did not completely eliminate autoproteolytic activity, suggesting that this substitution might not represent a *GPR126*-null allele. Nonetheless, the biochemical analysis and pedigree information together suggest that this allele causes a strong loss of GPR126 function. Thus, molecular and genetic studies support the conclusion that the mutations in these three families all cause AMC by reducing or eliminating GPR126 function.

In addition to playing a key role in myelination of the PNS, GPR126 has also been implicated in bone mineralization. Morpholino knockdown of *gpr126* in zebrafish gave results suggesting decreased mineralization of the vertebrae.[23] SNPs in *GPR126* have also been associated with idiopathic scoliosis[23,24] and skeletal-frame size and height.[24–26] In further support of a link between GPR126 and skeletal development, one individual presented here (II:2 in family 3) is also affected by vertebral anomalies.

Here, we thus present three consanguineous families affected by lethal arthrogryposis and homozygous loss-of-function mutations in *GPR126*. These data suggest

that *GPR126* mutations should be considered in individuals with AMC and add to the growing body of literature[5] implicating defective axoglial function as a key mechanism responsible for cases of severe AMC.

Accession Numbers

The accession numbers for the c.19C>T (p.Arg7*), c.2144dup (p.Gln716Thrfs*16), and c.2306T>A (p.Val769Glu) variants reported in this paper are ClinVar: SCV000222094, SCV000222095, and SCV000222096, respectively.

Supplemental Data

Supplemental Data include seven figures and can be found with this article online at http://dx.doi.org/10.1016/j.ajhg.2015.04.014.

Acknowledgments

This work was supported by the National Health and Medical Research Council of Australia (Early Career Researcher Fellowship 1035955 to G.R. and Research Fellowship APP1002147 and Project Grant APP1022707 to N.G.L.). This work was also supported by grants from the French Ministry of Health (Programme Hospitalier de Recherche Clinique 2010, AOM10181), the Association Française contre les Myopathies (DAJ1891), and INSERM and University Paris-Sud (ERM2013) to J.M. Work in the W.S.T. lab was supported by NIH grant NS050223. The authors would like to thank the Exome Aggregation Consortium (a full list of contributing groups can be found at http://exac.broadinstitute.org/about) and the groups that provided exome variant data for comparison: the Clinical Research Unit of Bicêtre Hospital, the Department of Clinical Research and Development of the Assistance Publique – Hôpitaux de Paris, and the NHLBI Grand Opportunity Exome Sequencing Project and its ongoing studies, which produced and provided exome variant calls for comparison.

Received: February 13, 2015
Accepted: April 20, 2015
Published: May 21, 2015

Web Resources

The URLs for data presented herein are as follows:

1000 Genomes, http://www.1000genomes.org
ANNOVAR, http://www.openbioinformatics.org/en/latest/
ClinVar, http://www.ncbi.nlm.nih.gov/clinvar/
Ensembl Genome Browser, http://www.ensembl.org/index.html
ExAC Browser, http://exac.broadinstitute.org
MutationTaster, http://mutationtaster.org
NHLBI Exome Sequencing Project (ESP) Exome Variant Server, http://evs.gs.washington.edu/EVS/
OMIM, http://www.omim.org/
PolyPhen-2, http://genetics.bwh.harvard.edu/pph2/
PROVEAN, http://provean.jcvi.org/index.php
SIFT, http://sift.jcvi.org
UCSC Human Genome Browser, http://genome.ucsc.edu/cgi-bin/hgGateway

References

1. Hall, J.G. (1997). Arthrogryposis multiplex congenita: etiology, genetics, classification, diagnostic approach, and general aspects. J. Pediatr. Orthop. B *6*, 159–166.
2. Haliloglu, G., and Topaloglu, H. (2013). Arthrogryposis and fetal hypomobility syndrome. Handb. Clin. Neurol. *113*, 1311–1319.
3. Hall, J.G. (1985). Genetic aspects of arthrogryposis. Clin. Orthop. Relat. Res. *194*, 44–53.
4. Gupta, V.A., Ravenscroft, G., Shaheen, R., Todd, E.J., Swanson, L.C., Shiina, M., Ogata, K., Hsu, C., Clarke, N.F., Darras, B.T., et al. (2013). Identification of KLHL41 Mutations Implicates BTB-Kelch-Mediated Ubiquitination as an Alternate Pathway to Myofibrillar Disruption in Nemaline Myopathy. Am. J. Hum. Genet. *93*, 1108–1117.
5. Laquérriere, A., Maluenda, J., Camus, A., Fontenas, L., Dieterich, K., Nolent, F., Zhou, J., Monnier, N., Latour, P., Gentil, D., et al. (2014). Mutations in CNTNAP1 and ADCY6 are responsible for severe arthrogryposis multiplex congenita with axoglial defects. Hum. Mol. Genet. *23*, 2279–2289.
6. McMillin, M.J., Beck, A.E., Chong, J.X., Shively, K.M., Buckingham, K.J., Gildersleeve, H.I., Aracena, M.I., Aylsworth, A.S., Bitoun, P., Carey, J.C., et al.; University of Washington Center for Mendelian Genomics (2014). Mutations in PIEZO2 cause Gordon syndrome, Marden-Walker syndrome, and distal arthrogryposis type 5. Am. J. Hum. Genet. *94*, 734–744.
7. Patel, N., Smith, L.L., Faqeih, E., Mohamed, J., Gupta, V.A., and Alkuraya, F.S. (2014). ZBTB42 mutation defines a novel lethal congenital contracture syndrome (LCCS6). Hum. Mol. Genet. *23*, 6584–6593.
8. Monk, K.R., Naylor, S.G., Glenn, T.D., Mercurio, S., Perlin, J.R., Dominguez, C., Moens, C.B., and Talbot, W.S. (2009). A G protein-coupled receptor is essential for Schwann cells to initiate myelination. Science *325*, 1402–1405.
9. Edelhoff, S., Villacres, E.C., Storm, D.R., and Disteche, C.M. (1995). Mapping of adenylyl cyclase genes type I, II, III, IV, V, and VI in mouse. Mamm. Genome *6*, 111–113.
10. Li, H., and Durbin, R. (2009). Fast and accurate short read alignment with Burrows-Wheeler transform. Bioinformatics *25*, 1754–1760.
11. Li, H., Handsaker, B., Wysoker, A., Fennell, T., Ruan, J., Homer, N., Marth, G., Abecasis, G., and Durbin, R.; 1000 Genome Project Data Processing Subgroup (2009). The Sequence Alignment/Map format and SAMtools. Bioinformatics *25*, 2078–2079.
12. Wang, K., Li, M., and Hakonarson, H. (2010). ANNOVAR: functional annotation of genetic variants from high-throughput sequencing data. Nucleic Acids Res. *38*, e164.
13. Robinson, J.T., Thorvaldsdóttir, H., Winckler, W., Guttman, M., Lander, E.S., Getz, G., and Mesirov, J.P. (2011). Integrative genomics viewer. Nat. Biotechnol. *29*, 24–26.
14. Yau, K.S., Allcock, R., Mina, K., Ravenscroft, G., Cabrera, M., Gooding, R., Wise, C., Sivadorai, P., Trajanoski, D., Atkinson, V., et al. (2014). G.P.18 Neurogenetic disease diagnostics by targeted capture and next generation sequencing. Neuromuscul. Disord. *24*, 799–800.
15. Monk, K.R., Oshima, K., Jörs, S., Heller, S., and Talbot, W.S. (2011). Gpr126 is essential for peripheral nerve development and myelination in mammals. Development *138*, 2673–2680.

16. Lyons, D.A., and Talbot, W.S. (2014). Glial Cell Development and Function in Zebrafish. Cold Spring Harb. Perspect. Biol. *7*, a020586.
17. Langenhan, T., Aust, G., and Hamann, J. (2013). Sticky signaling—adhesion class G protein-coupled receptors take the stage. Sci. Signal. *6*, re3.
18. Araç, D., Boucard, A.A., Bolliger, M.F., Nguyen, J., Soltis, S.M., Südhof, T.C., and Brunger, A.T. (2012). A novel evolutionarily conserved domain of cell-adhesion GPCRs mediates autoproteolysis. EMBO J. *31*, 1364–1378.
19. Paavola, K.J., Sidik, H., Zuchero, J.B., Eckart, M., and Talbot, W.S. (2014). Type IV collagen is an activating ligand for the adhesion G protein-coupled receptor GPR126. Sci. Signal. *7*, ra76.
20. Liebscher, I., Schön, J., Petersen, S.C., Fischer, L., Auerbach, N., Demberg, L.M., Mogha, A., Cöster, M., Simon, K.U., Rothemund, S., et al. (2014). A tethered agonist within the ectodomain activates the adhesion G protein-coupled receptors GPR126 and GPR133. Cell Rep. *9*, 2018–2026.
21. Glenn, T.D., and Talbot, W.S. (2013). Analysis of Gpr126 function defines distinct mechanisms controlling the initiation and maturation of myelin. Development *140*, 3167–3175.
22. Mogha, A., Benesh, A.E., Patra, C., Engel, F.B., Schöneberg, T., Liebscher, I., and Monk, K.R. (2013). Gpr126 functions in Schwann cells to control differentiation and myelination via G-protein activation. J. Neurosci. *33*, 17976–17985.
23. Kou, I., Takahashi, Y., Johnson, T.A., Takahashi, A., Guo, L., Dai, J., Qiu, X., Sharma, S., Takimoto, A., Ogura, Y., et al. (2013). Genetic variants in GPR126 are associated with adolescent idiopathic scoliosis. Nat. Genet. *45*, 676–679.
24. Xu, J.F., Yang, G.H., Pan, X.H., Zhang, S.J., Zhao, C., Qiu, B.S., Gu, H.F., Hong, J.F., Cao, L., Chen, Y., et al. (2015). Association of GPR126 gene polymorphism with adolescent idiopathic scoliosis in Chinese populations. Genomics *105*, 101–107.
25. Liu, J.Z., Medland, S.E., Wright, M.J., Henders, A.K., Heath, A.C., Madden, P.A., Duncan, A., Montgomery, G.W., Martin, N.G., and McRae, A.F. (2010). Genome-wide association study of height and body mass index in Australian twin families. Twin Res. Hum. Genet. *13*, 179–193.
26. Zhao, J., Li, M., Bradfield, J.P., Zhang, H., Mentch, F.D., Wang, K., Sleiman, P.M., Kim, C.E., Glessner, J.T., Hou, C., et al. (2010). The role of height-associated loci identified in genome wide association studies in the determination of pediatric stature. BMC Med. Genet. *11*, 96.